Electronic Supplementary Material (ESI) for ChemComm.

"Covalent immobilization of *N*-heterocyclic carbenes on pristine carbon substrates: from nanoscale characterization to bulk catalysis"

Brent Daelemans[1,2], Sven Bernaerts,[1] Samuel Eyley[3], Wim Thielemans[3], Wim Dehaen[2] and Steven De Feyter[1]

[1]*Division of Molecular Imaging and Photonics, Department of Chemistry, KU Leuven, Celestijnenlaan 200F, 3001 Leuven, Belgium*

[2]*Division of Sustainable Chemistry for Metals and Molecules, Department of Chemistry, KU Leuven, Celestijnenlaan 200F, 3001 Leuven, Belgium*

[3]*Sustainable Materials Lab, Department of Chemical Engineering, KU Leuven, campus Kulak Kortrijk, E. Sabbelaan 53, 8500 Kortrijk, Belgium*

Contents:

1. Synthesis procedures

General experimental procedure

4-Nitrophenethyl bromide (98%, TCI Europe NV), zinc dust (98%, Acros Organics NV), ammonium formate (98%, Merck Life Science BV), acetic anhydride (99%, VWR International BV), triethylamine (99%, Acros Organics NV), 1,2,4-triazole (99.5%, Acros Organics NV), methyl iodide (99%, Fisher Scientific Belgium BV), cesium carbonate (99.5%, Fisher Scientific Belgium BV), benzaldehyde (TCI Europe NV), thionyl chloride (99.5%, Acros Organics NV) and 2-phenethyl bromide (98%, Acros Organics NV) were bought from commercial suppliers. NMR spectra were acquired in DMSO-d_6, $CDCl_3$, D_2O or MeOD on a Bruker AMX 400 MHz and chemical shifts (δ) are reported in parts per million (ppm). The solvent peak of methanol (3.310 ppm, *q*, *J*= 1.7 Hz, 3H) or tetramethylsilane (0.000 ppm, s, 12H) was used as the reference peak. Melting points were determined using a Reichert Thermovar apparatus and are uncorrected. High-resolution mass spectra were acquired on a quadrupole orthogonal acceleration time-of-flight mass spectrometer (Synapt G2 HDMS, Waters, Milford, MA, USA). Samples were infused at 3 mL/min and spectra were obtained in positive ionization mode with a resolution of 15,000 FWHM (full width at half maximum) using leucine enkephalin as a lock mass.

Synthesis of *N*-[4-(2-Bromoethyl)phenyl]-acetamide (1):

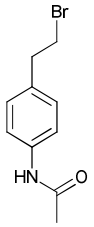

4-Nitrophenethyl bromide (10.00 g, 0.043 mol) and ammonium formate (11.94 g, 0.189 mol, 4.4 eq.) were dissolved in 130 mL methanol. Zn (17.05 g, 0.261 mol, 6 eq.) was added to a 250 mL round bottom flask (RBF) and activated with 1 M HCl (40 mL). After 5 minutes of stirring, HCl was removed from the Zn by decantation. 4-Nitrophenethyl bromide and ammonium formate solution were added and the mixture was stirred for 30 minutes at RT.[1] The mixture was filtered and the solvent evaporated. The residue was dissolved in 130 mL DCM and washed twice with $NaHCO_3$ and once with brine. The organic phase was collected and triethylamine (6.60 g, 0.065 mol, 1.5 eq.) and acetic anhydride (8.88 g, 0.087 mol, 2 eq.) were added. The reaction mixture was stirred for 48 hours at RT. After this time, the mixture was washed twice with saturated $NaHCO_3$ and once with brine, dried with $MgSO_4$. The solvent was evaporated, and the crude product was purified using column chromatography in petroleum ether/ethyl acetate (8/2) to give compound **1** (1.72 g, 0.007 mol, 16%) as a white powder.

^{1}H-NMR (400 MHz, $CDCl_3$):δ 7.45 (d, J = 8.3 Hz, 2H), 7.16 (d, J = 8.3 Hz, 2H), 3.54 (t, J = 7.6 Hz, 2H), 3.12 (t, J = 7.6 Hz, 2H), 2.17 (s, 3H). The ^{1}H-NMR spectrum is in agreement with a previous report.[2]

Synthesis of 1-methyl-1,2,4-triazole:

The synthesis of 1-methyl-1,2,4-triazole was performed by adapting a previously reported procedure.[3] In a 100 mL reaction tube, 1,2,4-triazole (1.00 g, 0.014 mol) was dissolved in THF (24 mL). Methyl iodide (1.33 mL, 0.021 mol) was added, and the mixture was stirred at RT for 24 hours. The reaction was stopped and an excess of NaOH was added. The salts were removed via filtration and the solvent was evaporated under reduced pressure. 1-Methyl-1,2,4-triazole was obtained after vacuum distillation (0.117 g, 10%) as a colorless oil.

^{1}H-NMR (400 MHz, $CDCl_3$): δ8.04 (s, 1H), 7.93 (s, 1H), 3.94 (s, 3H).

Synthesis of 4-(4-acetamidophenethyl)-1-methyl-4*H*-1,2,4-triazolium bromide (2):

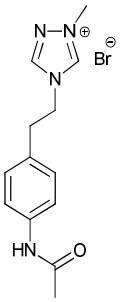

N-[4-(2-Bromoethyl)phenyl]-acetamide (**1**) (400 mg, 1.65 mmol) and 1-methyl-1,2,4-triazole (150 mg, 1.8 mmol) were dissolved in 2 mL THF in a 10 mL reaction tube. The mixture was stirred for 40 hours under reflux. The solution was cooled to room temperature. The precipitate was filtered and washed with THF. The residue was dried under reduced pressure to give compound **2** (0.243 g, 0.75 mmol, 45%) as a white powder.

^{1}H-NMR (400 MHz, DMSO-d_6): δ10.05 (s, 1H), 9.94 (s, 1H), 9.12 (s, 1H), 7.54 (d, 2H), 7.17 (d, 2H), 4.50 (t, 2H), 4.06 (s, 3H), 3.10 (t, 2H), 2.04 (s, 3H). ^{13}C-NMR (101 MHz, DMSO-d_6): δ168.22 (s, 1C), 144.51 (s, 1C), 142.76 (s, 1C), 138.25 (s, 1C), 130.72 (s, 1C), 128.96 (s, 2C), 119.15 (s, 2C), 48.38 (s, 1C), 38.69 (s, 1C), 34.35 (s,1C), 23.97 (s, 1C), *m.p.*: 224.5-225.5 °C, MS+: 245.1399, expected mass: 245.1402 m/z $[M-Br]^+$.

Synthesis of 4-(4-ammoniophenethyl)-1-methyl-4*H*-1,2,4-triazolium chloride (3):

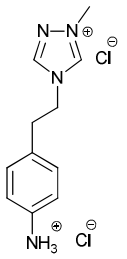

Compound **2** (0.320 g, 0.98 mmol) and thionyl chloride (0.36 mL, 4.92 mmol) were dissolved in 7 mL methanol in a 10 mL reaction tube.[4] The mixture was stirred for 20 hours at 70 °C. The solvent was evaporated under reduced pressure. The residue was extracted with 1 M NaOH and DCM. The aqueous phase was acidified with HCl and extracted with ethyl acetate. The aqueous phase was evaporated under reduced pressure. The residue was dispersed in methanol and filtered to remove rests of salt present. The filtrate was dried under reduced pressure and purified using reverse HPLC using a water/methanol mixture as eluent 1/0 => 5/5 to give compound **3** (0.087 g, 32%) as a yellow powder.

^{1}H-NMR (400 MHz, D_2O, MeOH): δ9.67 (s, 1H), 8.68 (s, 1H), 7.40 (m, 4H), 4.66 (t, 2H), 4.10 (s, 3H), 3.31 (t, 2H). ^{13}C-NMR (101 MHz, D_2O, MeOH): δ 145.00 (s, 1C), 142.84 (s, 1C), 137.92 (s, 1C), 131.15 (s, 2C), 129.65 (s, 1C), 124.22 (s, 2C), 49.58 (s, 1C), 39.33 (s, 1C), 35.32 (s, 1C), *m.p.*: 233-235 °C, MS+: 221.1398 m/z expected mass: 221.14022 m/z $[M\text{-}HCl\text{-}Cl+H_2O]^+$.

Synthesis of 1-methyl-4-phenethyl-1,2,4-triazolium bromide (5):

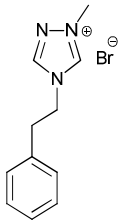

2-Phenylethylbromide (240 mg, 1.3 mmol) and 1-methyl-1,2,4-triazole (120 mg, 1.4 mmol) were dissolved in 2 mL THF in a 10 mL reaction tube. The mixture was stirred for 72 hours under reflux. The solution was cooled to room temperature. The precipitate was filtered and washed with THF. The residue was dried under reduced pressure to give compound **5** (0.051 g, 0.2 mmol, 15%) as a white powder.

^{1}H-NMR (400 MHz, MeOD): δ9.83 (s, 1H), 8.83 (s, 1H), 7.37-7.31 (m, 2H), 7.31-7.24 (m, 1H), 7.25-7.21 (m, 2H), 4.58 (t, *J*=7.3 Hz, 2H), 4.10 (s, 3H), 3.23 (t, *J*=7.3 Hz, 2H). ^{13}C-NMR (101 MHz, MeOD): δ145.68 (s, 1C), 137.28 (s, 1C), 130.12 (s, 2C), 129.89 (s, 2C), 128.56 (s, 1C), 50.45 (s, 1C),

39.39 (s, 1C), 36.75 (s, 1C). *m.p.*: 139-141 °C, MS+: 188.1178, expected mass: 188.11876 m/z [M-Br]$^+$.

2. Grafting and characterization of NHC-precursors on carbon substrates

General experimental procedure

HOPG: A solution of 20 mM NHC-precursor **3** and 20 mM $NaNO_2$ was made in 40 mM HCl to form the corresponding diazonium salt. The success of the reaction was tested by performing the reaction in D_2O, followed by characterization by ^{1}H-NMR which showed a clear change in the chemical shift of the peaks in the aromatic region (Figure S22).

A 20 mM solution of ascorbic acid was made in 50 mM KOH. First, 100 µL of the ascorbic acid solution was added to a freshly cleaved HOPG substrate (HOPG, grade ZYB, Advanced Ceramics Inc., Cleveland, OH, U.S.A.), followed by 100 µL of the precursor solution. The sample was left for 10 minutes at room temperature and was washed afterwards with acetonitrile and MilliQ water. The samples were dried under a stream of air and characterized with different surface characterization techniques.

Graphitic powder: GNP (91 at.% C, thickness 1-4 nm) was obtained from PlasmaChem.

A 10 mL solution of 20 mM NHC-precursor **3** and 20 mM $NaNO_2$ was made in 40 mM HCl to form the corresponding diazonium salt. A 10 mL solution of 20 mM ascorbic acid was made in 50 mM KOH. First, 20 mg of GNP were dispersed in the ascorbic acid solution and sonicated for 30 minutes. Next, the solution containing the NHC-precursor was added and the mixture was stirred overnight. The resulting mixture was centrifuged for 35 min at 8500 rpm and decanted. The powder was washed 1 time with MilliQ water and 2 times with acetonitrile and dried in a vacuum oven.

2.1 Characterization techniques

Atomic force microscopy

AFM imaging was performed with a Multimode 8 (Bruker) with a Nanoscope V controller. OMCL-AC240TS-R3 probes (spring constant ~2 N/m) with a resonance frequency around 70 kHz were used. Data analysis was done using SPIP software (Image Metrology A/S). Scratching experiments where performed by selecting a 0.5×0.5 µm domain and increasing the setpoint to 1.7 V. After scanning up and down for 5 times, the setpoint was decreased to 0.2 V, and the image was zoomed out to 2×2 µm. The height of the monolayer was averaged over 14 height values from 3 different images, of which each height value was averaged over 25 lines. The error shown is the standard deviation calculated over these values.

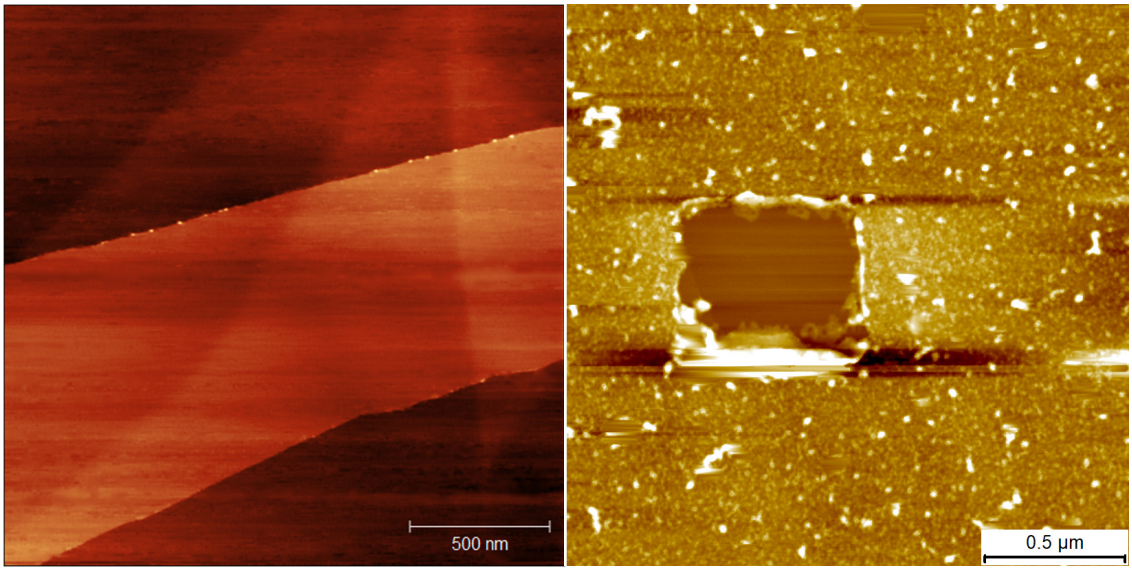

Figure S1*. 2×2 µm AFM images of a blank (left) and functionalized (right) HOPG substrate. A clean, uniform surface is observed which is in contrast with the granular structure that is observed for the functionalized HOPG sample.*

Atomic force microscopy-infrared spectroscopy (AFM-IR)

As FTIR in bulk was troublesome due to a high background noise of the graphite itself, AFM-IR measurements on functionalized HOPG were performed. AFM-IR measurements in tapping mode were conducted using a nanoIR3-s system equipped with a Bruker Hyperspectral QCL laser source emitting in the mid-infrared range (934-1934 cm^{-1}). The pulse rate was set to the difference between the first and second cantilever eigenmodes. The first mode was utilized for tapping topography feedback, while the second mode was employed for IR detection (heterodyne force microscopy). AFM-IR measurements were performed using gold-coated silicon probes (PR-EX-TnIR-A-10) with a nominal diameter of approximately 25 nm, a resonance frequency of 60 kHz, and spring constant values of 2 N/m at the second eigenmode of approximately 400 kHz.

The characteristic bands of the triazolium unit (1582 cm^{-1} and 1161 cm^{-1}, see below 'infrared spectroscopy in bulk') can also be observed on the AFM-IR spectrum of the functionalized HOPG, which confirms the successful functionalization of HOPG. Other significant peaks in the AFM-IR spectrum can arise from C-C stretching in the aromatic ring (~1500 cm^{-1}) and ascorbic acid (~1322 cm^{-1}).[5] However, as the grafting structure is only a bilayer, the resolution that can be obtained with AFM-IR remains limited.

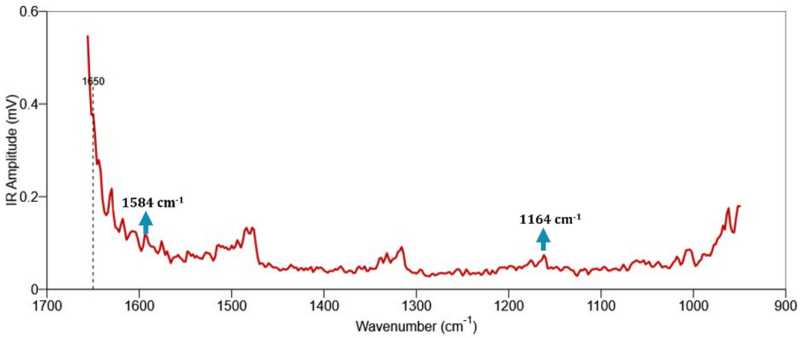

***Figure S2**. AFM-IR spectrum with two characteristic bands (1164 cm^{-1} and 1584 cm^{-1}) of the triazolium unit.*

Scanning tunneling microscopy

Scanning tunneling microscopy (STM, Pico SPM, Agilent) measurements were performed in constant current mode at the liquid-solid interface after addition of a droplet of 1-phenyloctane at room temperature (20-25 °C). Mechanically cut Pt/Ir wire (80/20, 0.25 mm diameter) were used as STM tips. Analysis was done using SPIP software (Image Metrology A/S).

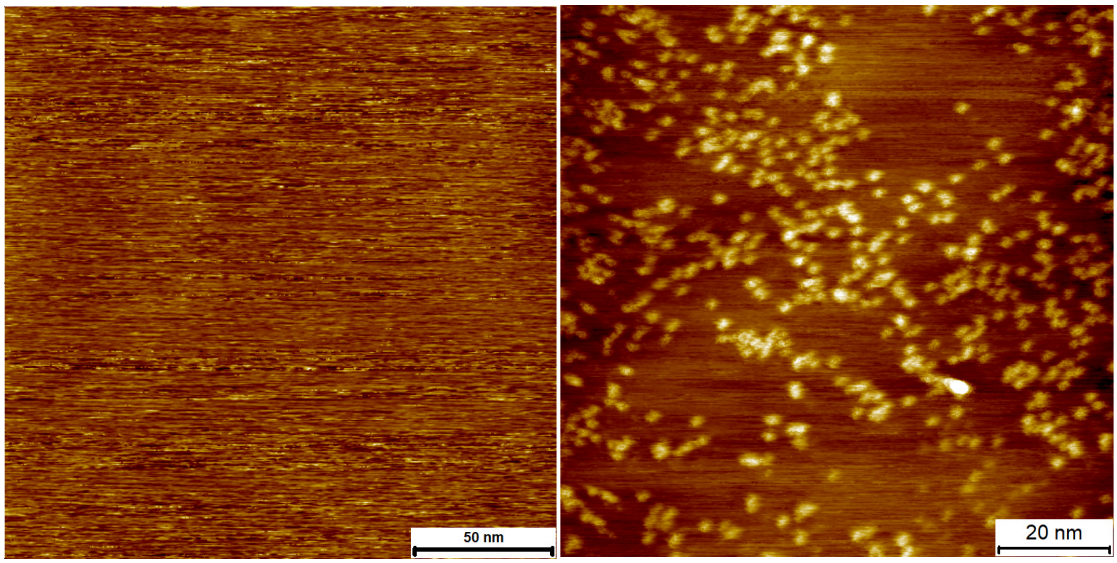

***Figure S3**. STM image of a blank HOPG substrate (left): 200×200 nm, I_{set} = 0.030 nA, V_{bias} = -0.900 V, and a functionalized HOPG substrate (right): 100×100 nm, I_{set} = 0.030 nA, V_{bias} = -0.900 V. No bright dots are observed on the blank sample, which indicates that the appearance of the bright dots is caused by covalent functionalization, as was reported before.*[6]

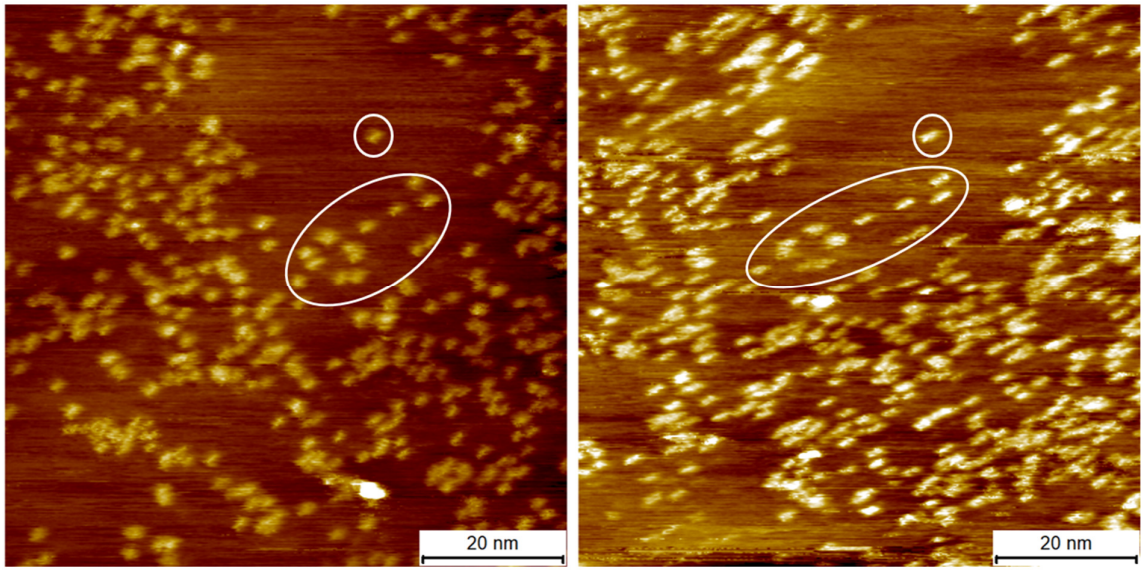

Figure S4*. Consecutive images in the STM after the grafting experiment. The same patterns are observed in both scans, which shows the anchored nature of the molecules. Scanning conditions: 100×100 nm,* I_{set} *= 0.030 nA,* V_{bias} *= -0.900 V.*

Raman spectroscopy

Raman spectra were collected with a confocal Raman microscope (Monovista CRS+, S&I GmbH) using a 532 nm He–Ne laser directed on the surface through an objective (OLYMPUS, BX43 50x, N.A. 0.7) with an optical density at the sample surface of about 590 kW cm^{-2}. The Raman scattering was collected using the same objective and guided to a Raman spectrograph (S&I GmbH) equipped with a cooled-charge coupled device (CCD) camera operated at -100 °C (Andor Technology, DU920P-BX2DD). All measurements were carried out under ambient conditions at room temperature.

HOPG: Accumulation time for all spectra was 100 s (5 s exposure time, 20 acquisitions). Analysis of the I_D/I_G ratio was performed using Igor software (Wavemetrics). Raman spectra were taken in at least 25 different positions on the sample. When the spectra of the blank and functionalized HOPG are compared, a clear appearance of a D band (~1330 cm^{-1}) can be observed for the functionalized HOPG.

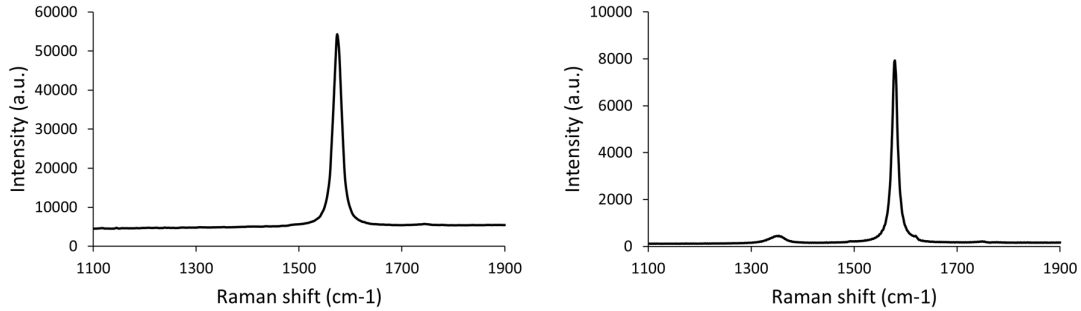

Figure S5*. Raman spectra of the pristine HOPG (left) and the functionalized GNP (right).*

Graphitic powder: The graphitic powders were dispersed in acetonitrile (1 mg mL^{-1}) and drop-casted on a silicon wafer. Accumulation time for all spectra was 250 s (5 s exposure time, 50 acquisitions). Raman spectra were taken in at least 20 different positions on the sample. The Raman spectra were corrected using a blank of the silicon wafer and fitted to sums of functions using Origin 9.8 software. Four Lorentz functions were used for deconvolution of the Raman peaks for respectively D"(~1200 cm^{-1}), D (~1330 cm^{-1}), D* (~1500 cm^{-1}), G (~1585 cm^{-1}), and D' (~1620 cm^{-1}) bands. The areas of the peaks were used for calculation of the I_D/I_G ratio and the standard deviation.

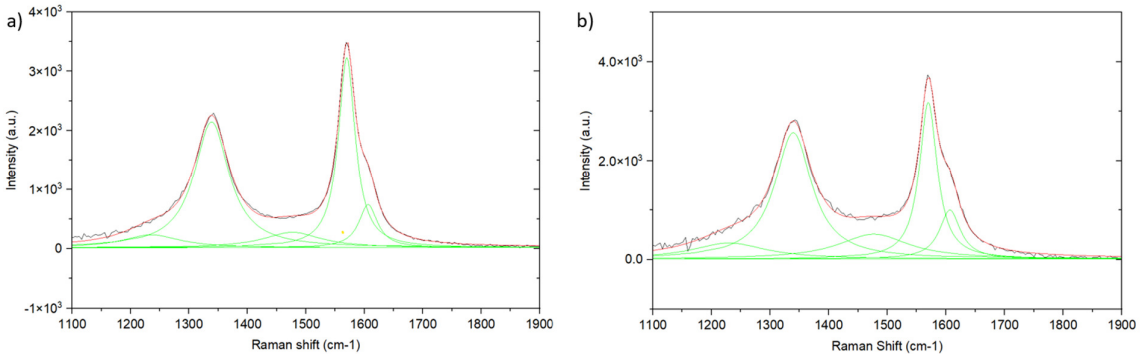

Figure S6*. Raman spectra of the a) non-functionalized GNP, and b) functionalized GNP. One spectrum is shown for each sample. Five Lorentz functions were used for deconvolution of the Raman spectra for respectively D" (~1200 cm^{-1}), D (~1330 cm^{-1}), D* (~1500 cm^{-1}), G (~1585 cm^{-1}), and D' (~1620 cm^{-1}) bands.*

X-ray photoelectron spectroscopy

X-ray photoelectron spectra were collected using a Kratos Axis Supra photoelectron spectrometer with a monochromated Al Kα X-ray source ($h\nu$ = 1486.7 eV, 120 W). Samples were mounted isolated from the spectrometer and charge neutralized using a low energy electron gun within the field of the magnetic lens. Spectra were recorded using hybrid (electrostatic/magnetic) optics with a slot aperture (700 µm × 300 µm). The analyzer was operated in fixed analyzer transmission

(FAT) mode with survey scans taken at 160 eV pass energy, and high-resolution scans at 20 eV pass energy. Binding energy was referenced to the GNP C 1s maximum (graphitic carbon) measured previously on unmodified GNP in electrical contact with the spectrometer at 284.36 eV.

Data analysis was performed using CasaXPS version 2.3.25.[7] Peak areas were converted to equivalent homogeneous composition[8] using relative sensitivity factors (RSFs) based on Scofield photoelectron cross-sections with angular distribution correction for a source-analyser angle of 60°. Escape-depth correction was performed using the electron attenuation length according to Seah.[9] Data was corrected for the instrument intensity-energy response function using an NPL transmission function.[10] This combination of relative sensitivity factors and escape depth correction assumes homogeneous composition within the information depth of the XPS experiment. No corrections were performed for the potential presence of overlayer contamination or matrix effects, and the resulting elemental concentrations should be considered the homogeneous equivalent composition.

The increase in the elemental composition of positively charged nitrogen and chlorine shows the presence of the grafted triazolium moiety on GNP (Table S1 and Table S2). The XPS characterization of the blank powder was taken from a previous report by our group.[11] Additionally, the nitrogen peak was deconvoluted in Figure S7a, showing the expected ratio of positively charged nitrogen and C=N*-N bound nitrogen (2/1) for the triazolium moiety.

The catalytic loading of the catalyst was calculated by the amount of positively charged nitrogen as one grafted triazolium molecule contains two positively charged nitrogens. The relative amount of positively charged nitrogen atoms was divided by 2 to correct for the two positively charged nitrogens in each triazolium moiety (eq. 1). Additionally, to determine the catalytic loading as an amount of mol catalyst per gram GNP, the relative amount of N^+ should be divided by the molar mass of GNP. The molar mass of GNP was calculated by taking into account the relative amounts of all different atoms present and their respective molar masses. The presence of hydrogen in the material was neglected in the calculation of the catalytic loading.

$$Catalytic\ loading = \frac{Relative\ amount\ of\ N^{+} in\ GNP\ (\frac{mol\ N^{+}}{mol\ GNP})}{2 * M_{GNP}(\frac{g\ GNP}{mol\ GNP})} = 1.0\ \pm 0.5\ \frac{mmol}{g} \qquad (1)$$

After using the functionalized powder as a catalyst in the benzoin condensation, XPS characterization was performed again (Figure S7b). A clear decrease in the presence of positively charged nitrogen species can be observed, together with the formation of a neutral amine peak. This change can be caused by the degradation of the molecule where the triazolium group is removed from the molecule and triazole moieties are formed.

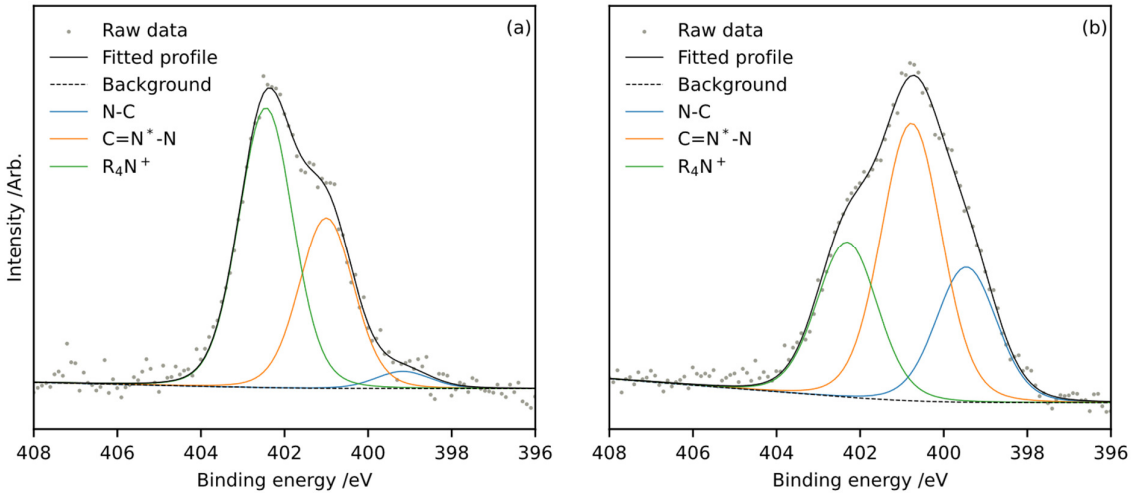

Figure S7*. XPS nitrogen 1s spectra of the functionalized carbon substrate a) before and b) after its use as a catalyst in benzoin condensation.*

Table S1. *Summary of the equivalent homogeneous composition according to XPS for different graphitic samples. Values of GNP were taken from previously performed and reported measurements on this powder.*[5]

	Carbon content (at%)	**Oxygen content (at%)**	**Nitrogen content (at%)**	**Fluorine content (at%)**	**Chlorine content (at%)**	**Bromine content (at%)**	**Silicon content (at%)**
Orbital	C 1s	O 1s	N 1s	F 1s	Cl 2p	Br 3d	Si 2p
RSF	1.00	2.93	1.80	4.43	2.18	2.70	0.77
GNP	91.8 ±1.2	7.6 ±1.2	0.45 ±0.05	/	0.13 ±0.04	/	0.04 ±0.06
Triazolium	83.1 ±2.5	10.2 ±5.6	4.5 ±2.2	/	1.0 ±0.4	0.2 ±0.1	1.0 ±0.1
Triazolium after reaction	85.5 ±0.1	8.5 ±0.5	4.2 ±0.9	0.8 ±0.4	0.7 ±0.1	/	0.3 ±0.1

Table S2. *Composition of different nitrogen environments determined from XPS high resolution spectra.*

	N-C (at%)	**C=N*-N (at%)**	**R_4N^+ (at%)**
Triazolium	0.26 ± 0.16	1.6 ± 0.76	2.63 ± 1.25
Triazolium after reaction	1.02 ± 0.23	2.0 ± 0.42	1.14 ± 0.26

Dispersibility experiment

The functionalized and non-functionalized GNP (1 mg) were dispersed in a mixture of deionized water (1 mL) and toluene (1 mL). The vials were shaken vigorously and the dispersions where allowed to stabilize for 5 minutes. Afterward, it was determined if the different graphitic powders favored the polar (water) or apolar (toluene) environment.

Infrared spectroscopy in bulk

Fourier transform infrared spectroscopy (FT-IR) was performed on a Vertex 70 (Bruker) via attenuated total reflectance (ATR). For each measurement, 64 scans were taken with a resolution of 2 cm^{-1}. The blank was recorded using using the atmosphere as background noise. Compound **3** was measured to determine if similar peaks were observed on HOPG and GNP. Characteristic peaks of the triazolium unit include the adsorption peaks at 1582 cm^{-1} and 1161 cm^{-1} (Figure S8), which are related to respectively the C=N vibration of triazolium group and the C-N vibration between the nitrogens of the triazolium and the carbons of the alkyl groups.[12-14]

The IR experiments on the bulk GNP did not give any results due to the significant absorption of the GNP itself (Figure S9). For this reason, AFM-IR was performed on functionalized HOPG to determine if the characteristic bands were present (see above: Atomic force microscopy-infrared spectroscopy). As the success of the grafting experiment is confirmed on the nanoscale, we hypothesize that a similar behavior can be expected on the bulk scale.

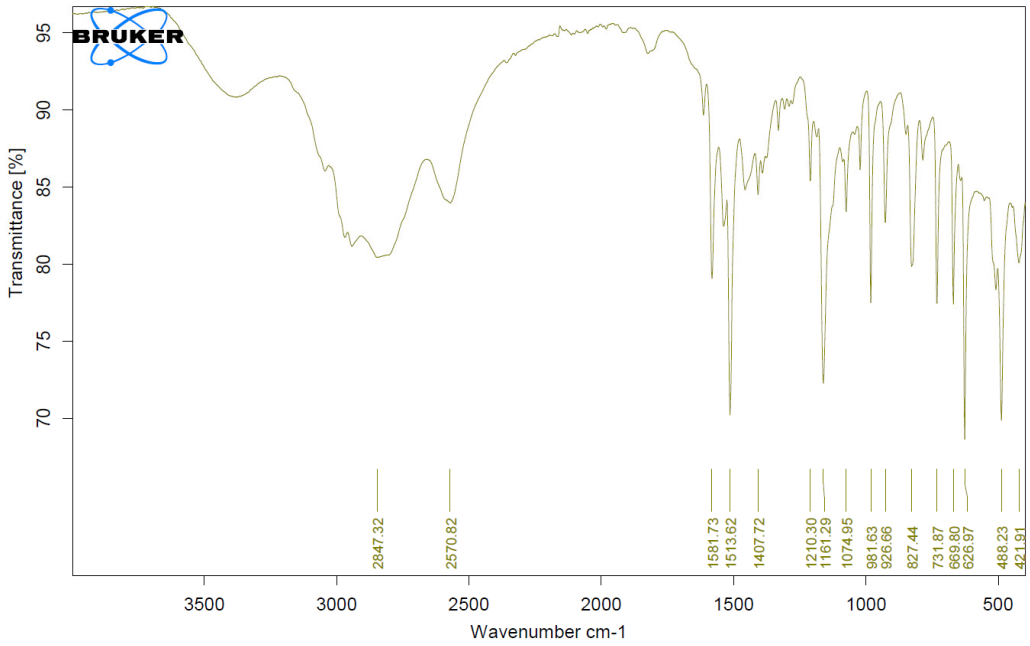

***Figure S8**. IR spectra of compound **3**.*

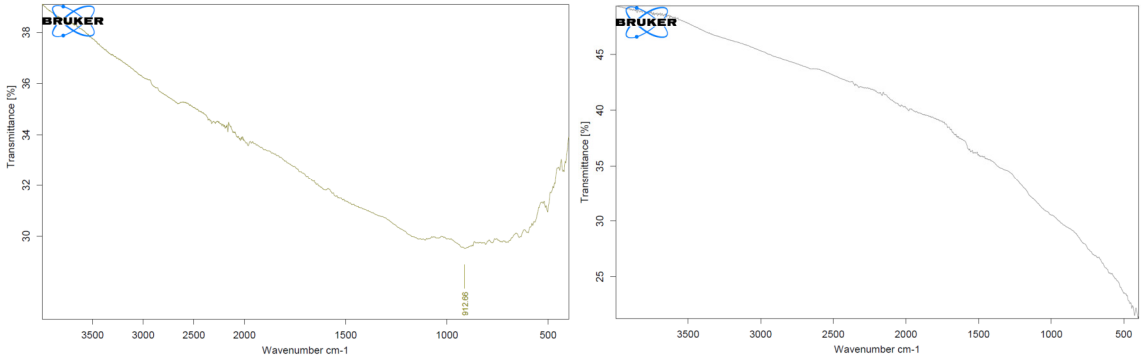

***Figure S9**. IR spectra of pristine GNP (left) and functionalized GNP (right). Due to the significant background signals from GNP itself, no characteristic molecular peaks of the grafted molecule can be observed.*

2.2 Catalysis experiments

The benzaldehyde used for the benzoin condensation was distilled before use and the reaction tubes were flame-dried. Four reaction tubes were used for the experiment: i) to the first, no additional catalyst was added, ii) to the second, 5 mg of pristine GNP was added, iii) to the third tube, 5 mg of the functionalized powder was added, and iv) to the fourth, compound **5** (1.6 mg, 0.006 mmol) was added. To each of these reaction tubes, 20 mol% cesium carbonate (13 mg, 0.04 mmol) was added. The reaction tubes were evacuated twice and backfilled with nitrogen. In a separate flask, benzaldehyde (0.120 mL, 1.2 mmol) and 1,3,5-trimethoxybenzene (20.2 mg,

0.12 mmol), as internal standard, were dissolved in 3 mL dry THF. The THF solution (0.5 mL) was added to the reaction vials, which means that 0.2 mmol benzaldehyde and 0.02 mmol 1,3,5-trimethoxybenzene were added to each reaction tube. The reaction was stirred for 24 hours at room temperature. Afterward, the reaction was stopped by adding 2 mL of 1 M HCl. The mixture was extracted by addition of ethyl acetate and the organic phase was taken and evaporated. The residue was dissolved in deuterated chloroform and the yield was calculated using ^{1}H-NMR via the internal standard peak of 1,3,5-trimethoxybenzene (6.03 ppm). The results of the catalytic experiments are summarized in Table S3.

For the recycling experiment, the powder was regained via centrifugation and washed 3 times with acetonitrile. The powder was dried overnight under vacuum and reused under the same reaction conditions as described above. However, no benzoin formation was observed which could be caused by the degradation of the grafted species under basic conditions. Since the triazolium group is a good leaving group, the strong basic medium during the reaction could cause ß-elimination.[15] In this reaction, the triazolium group is removed, and a styrene type molecule is formed (Scheme S1). The formation of this molecule would deactivate the catalyst and would prevent recycling of the graphitic powder. A possible solution would be to change the ethyl chain between the thiazolium or triazolium group to a longer, shorter, or branched chain to limit the amount of elimination that takes place. The stability of the molecule itself in basic medium was also tested as discussed below.

Table S3. *Summary of the catalytic experiments.*

Powder	**Yield**
None (blank)	0 %
GNP	0 %
Funct. GNP	17 %
Recycled Funct. GNP	0 %
Homogeneous Catalyst **5**	93 %

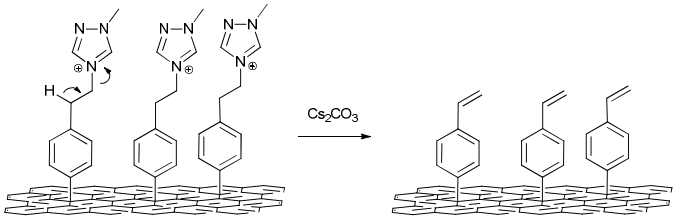

Scheme S1. *Proposed mechanism of degradation under basic conditions*

Stability experiments in basic medium

The reaction tubes were flame-dried. Two reaction tubes were used for the experiment: i) to the first, no base was added, ii) to the second, cesium carbonate (13 mg, 0.040 mmol) was added. To both reaction tubes, compound **3** (1.7 mg, 0.006 mmol) was added. The reaction tubes were evacuated twice and backfilled with nitrogen. In a separate flask, 1,3,5-trimethoxybenzene (20.2 mg, 0.12 mmol), as internal standard, was dissolved in 3 mL dry THF. The THF solution (0.5 mL) was added to the reaction vials, which means that 0.02 mmol 1,3,5-trimethoxybenzene was added to each reaction tube. The reaction was stirred for 24 hours at room temperature. Afterward, the reaction mixture was filtered and washed with methanol. The filtrate was taken and evaporated under reduced pressure at room temperature. The residue was dissolved in deuterated methanol and characterized by ^{1}H-NMR.

The two different spectra are compared in Figure S10. In the spectrum of the blank (red), the characteristic peaks of compound **3** can easily be distinguished. In the spectrum of the experiment in presence of base (blue), the characteristic peaks of the triazolium moieties are no longer observed. From this experiment, we can conclude that the grafted moieties are not stable under the strongly basic reaction conditions of the benzoin condensation and a more suitable molecular structure should be designed.

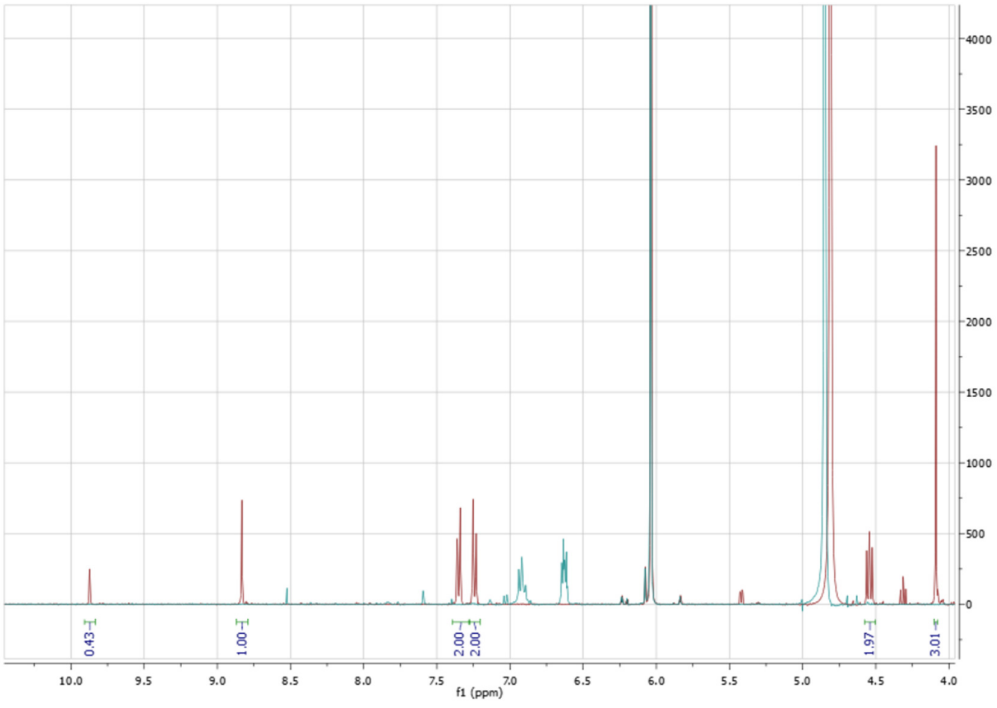

Figure S10. *^{1}H-NMR spectra of compound **3** stirred in neutral (red) or in basic (blue) conditions. The characteristic peaks can be observed after stirring in neutral conditions but cannot be observed after stirring in basic conditions.*

The same experiment was performed with compound **5** to inhibit degradation caused by the amine functionality present in compound **3**. Similarly, to compound **3**, the characteristic peaks are not present after stirring in basic medium (Figure S11). This experiment confirms the degradation of the triazolium moieties during the catalytic experiments.

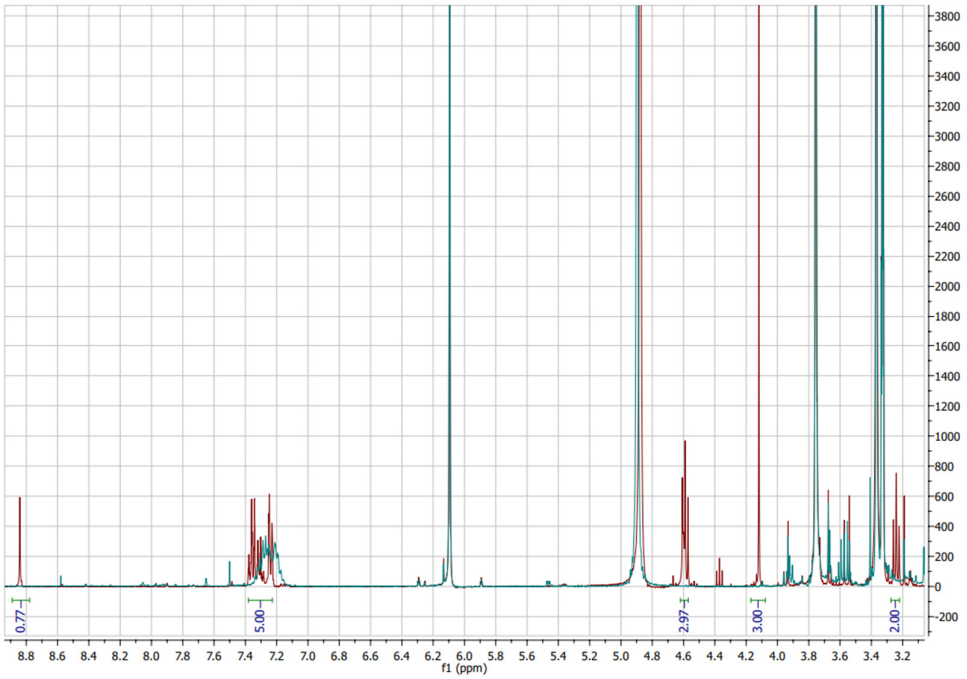

Figure S11. *^{1}H-NMR spectra of compound **5** stirred in neutral (red) or in basic (blue) conditions. The characteristic peaks can be observed after stirring in neutral conditions but cannot be observed after stirring in basic conditions.*

3. Spectra

Reference ^{1}H-NMR spectrum of compound 1 (400 MHz, $CDCl_3$):

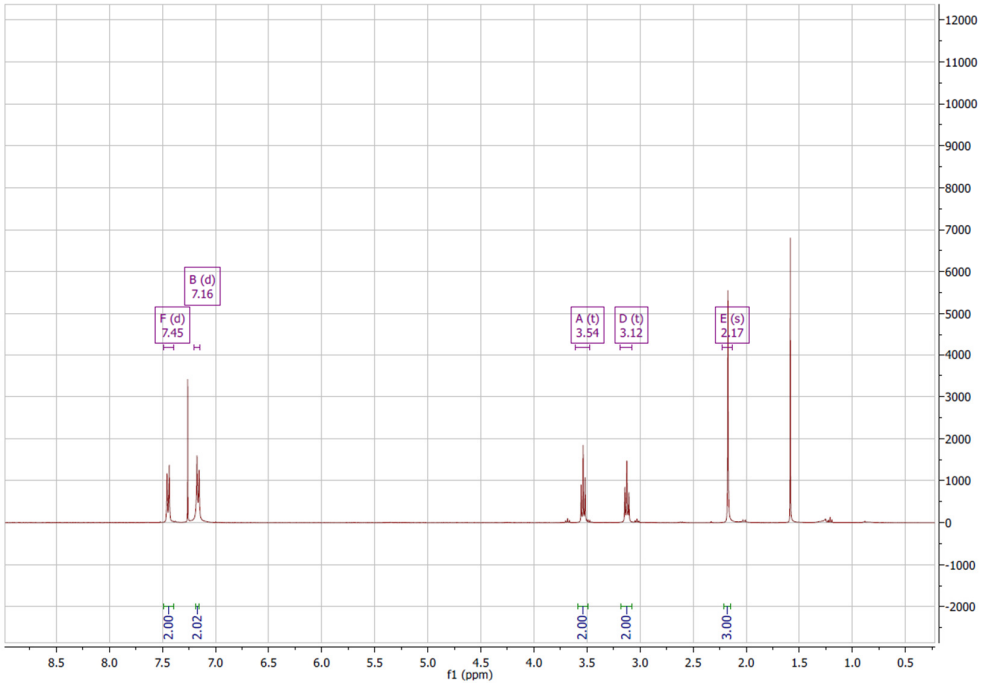

***Figure S12**. ^{1}H-NMR spectrum of compound **1** in $CDCl_3$.*

Reference ^{1}H-NMR spectrum of compound 2 (400 MHz, DMSO-d_6):

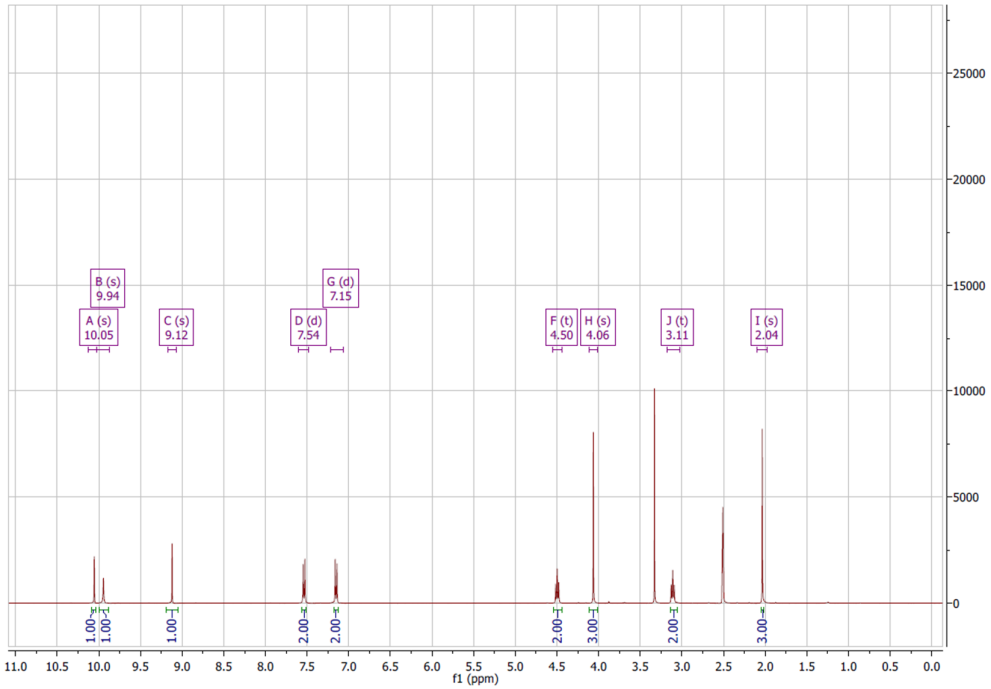

***Figure S13**. ^{1}H-NMR spectrum of compound **2** in DMSO-d_6.*

Reference ^{13}C-NMR spectrum of compound 2 (101 MHz, DMSO-d_6):

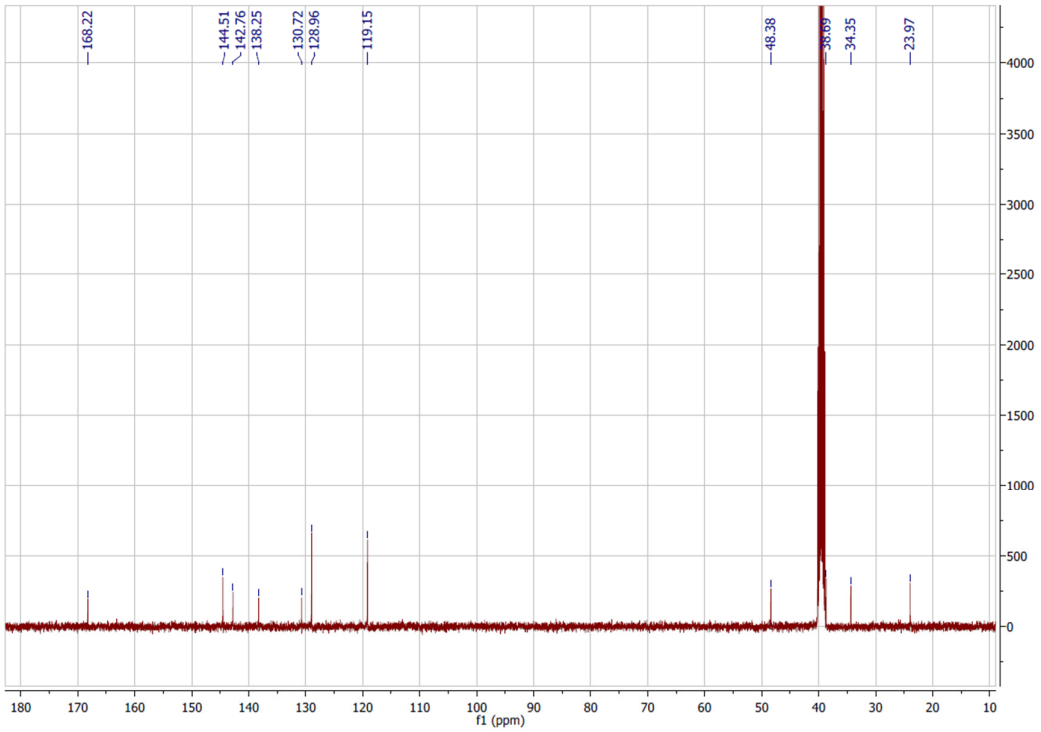

***Figure S14**. ^{13}C-NMR spectrum of compound **2** in DMSO-d_6.*

Reference HRMS spectrum of compound 2:

***Figure S15**. HRMS spectrum of compound **2**.*

Reference ^{1}H-NMR spectrum of compound 3 (400 MHz, D_2O):

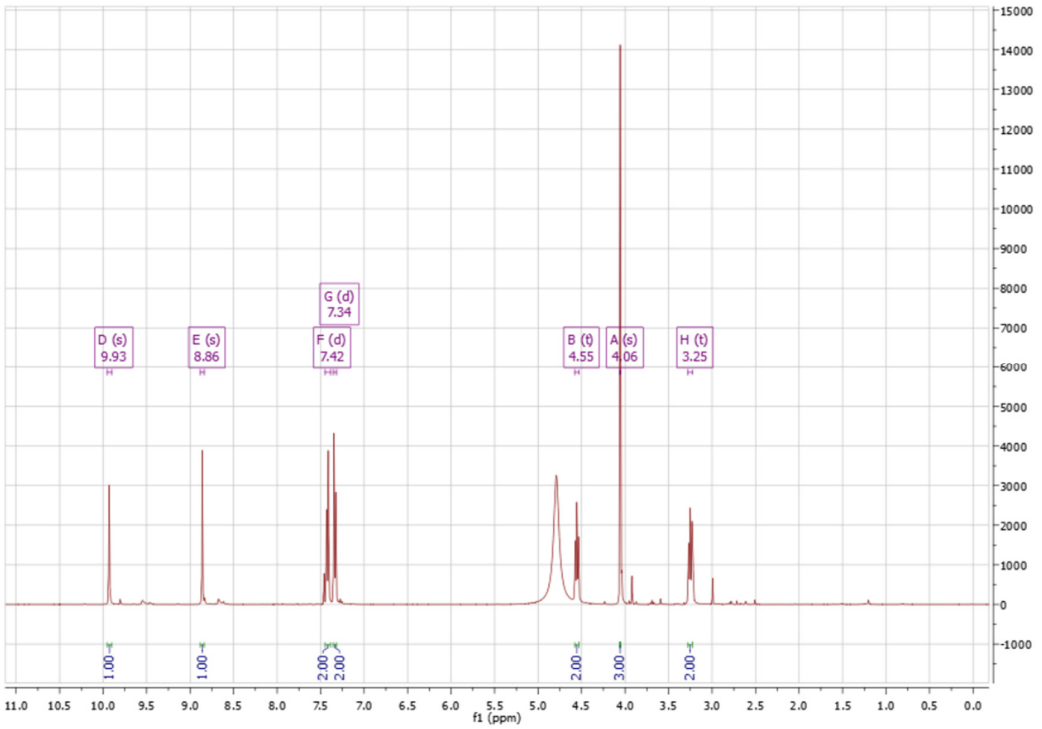

Figure S16. *^{1}H-NMR spectrum of compound **3** in D_2O.*

Reference ^{13}C-NMR spectrum of compound 3 (101 MHz, MeOD):

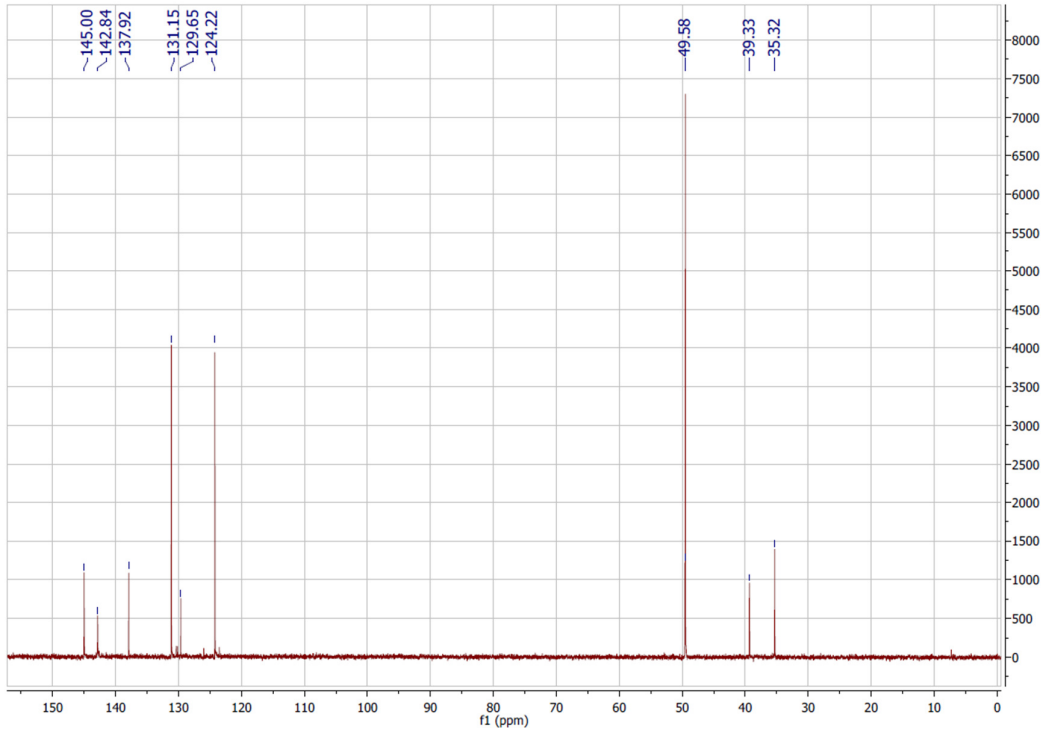

Figure S17. *^{13}C-NMR spectrum of compound **3** in MeOD.*

Reference HRMS spectrum of compound 3:

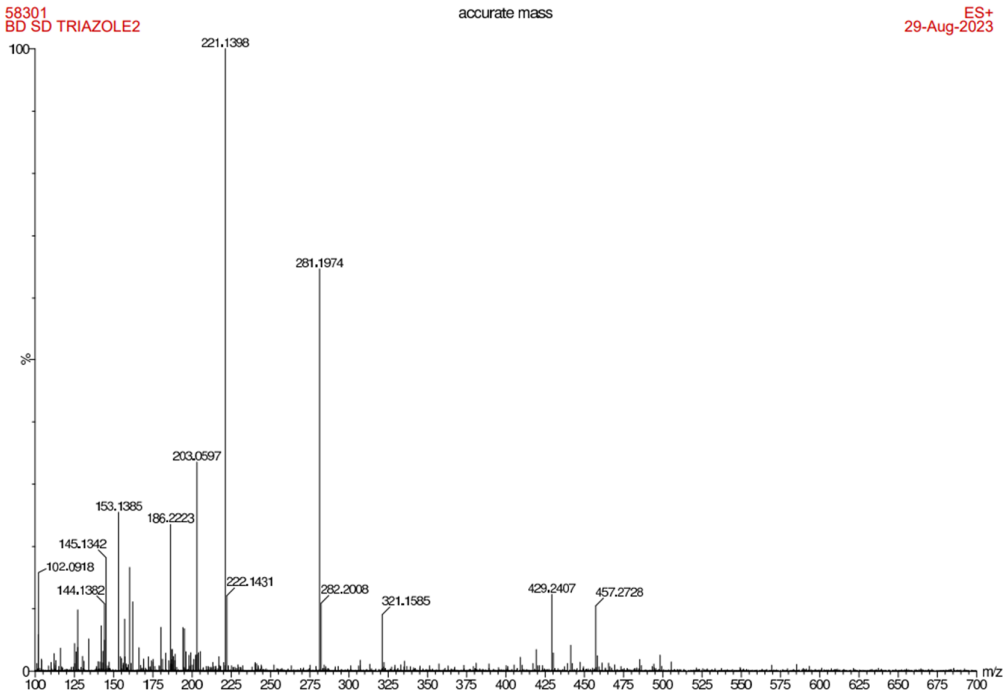

***Figure S18**. HRMS spectrum of compound **3**.*

Reference ^{1}H-NMR spectrum of compound 5 (400 MHz, MeOD):

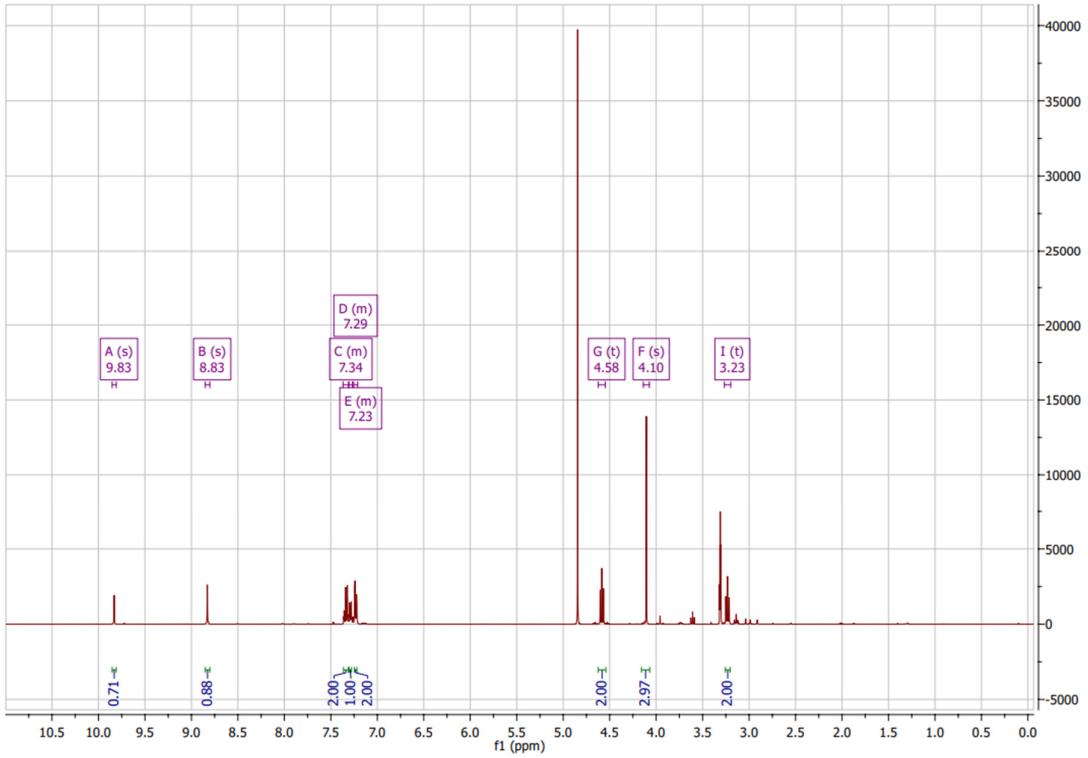

***Figure S19**. ^{1}H-NMR spectrum of compound **5** in MeOD.*

Reference ^{13}C-NMR spectrum of compound 5 (101 MHz, MeOD):

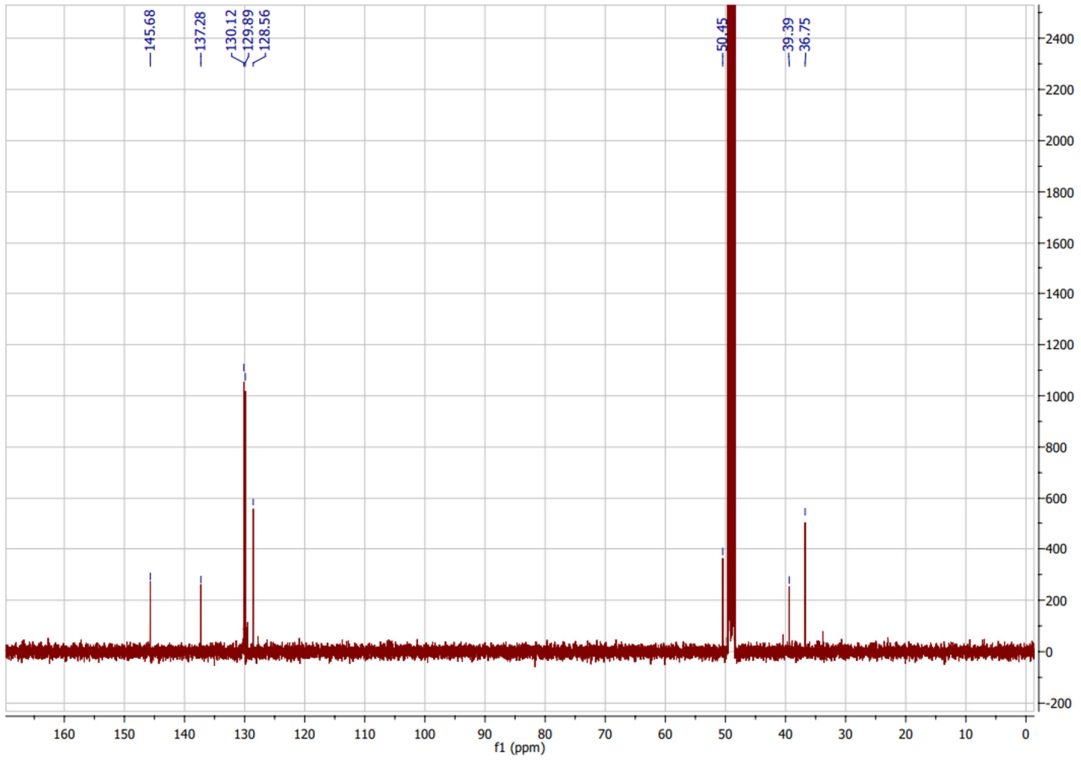

Figure S20. *^{13}C-NMR spectrum of compound **5** in MeOD.*

Reference HRMS spectrum of compound 5:

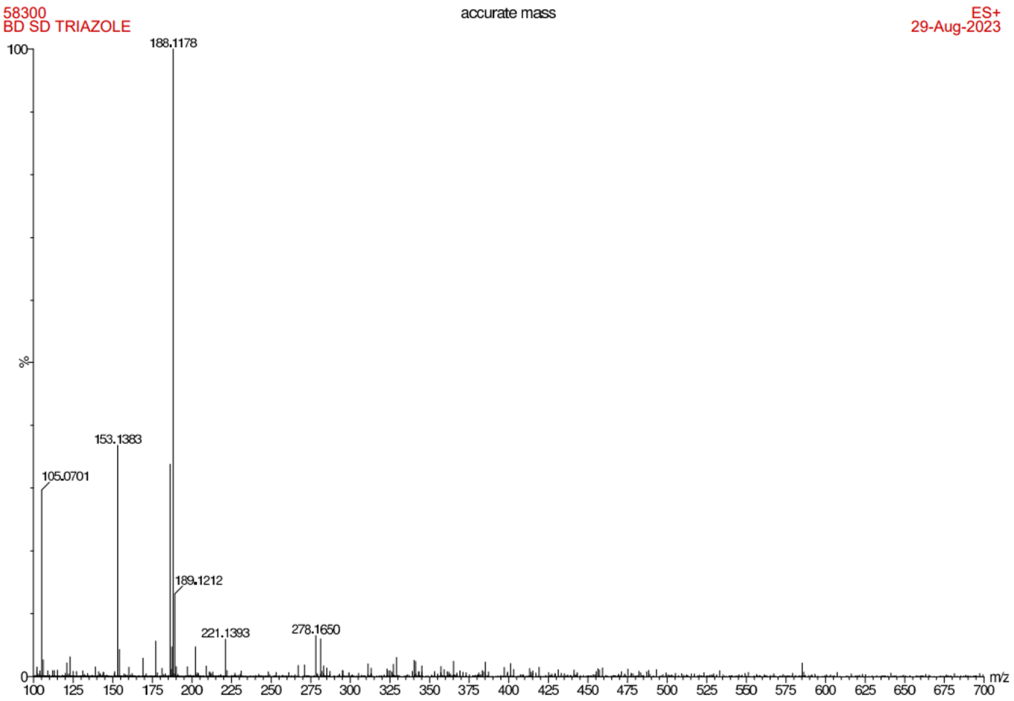

Figure S21. *HRMS spectrum of compound **5**.*

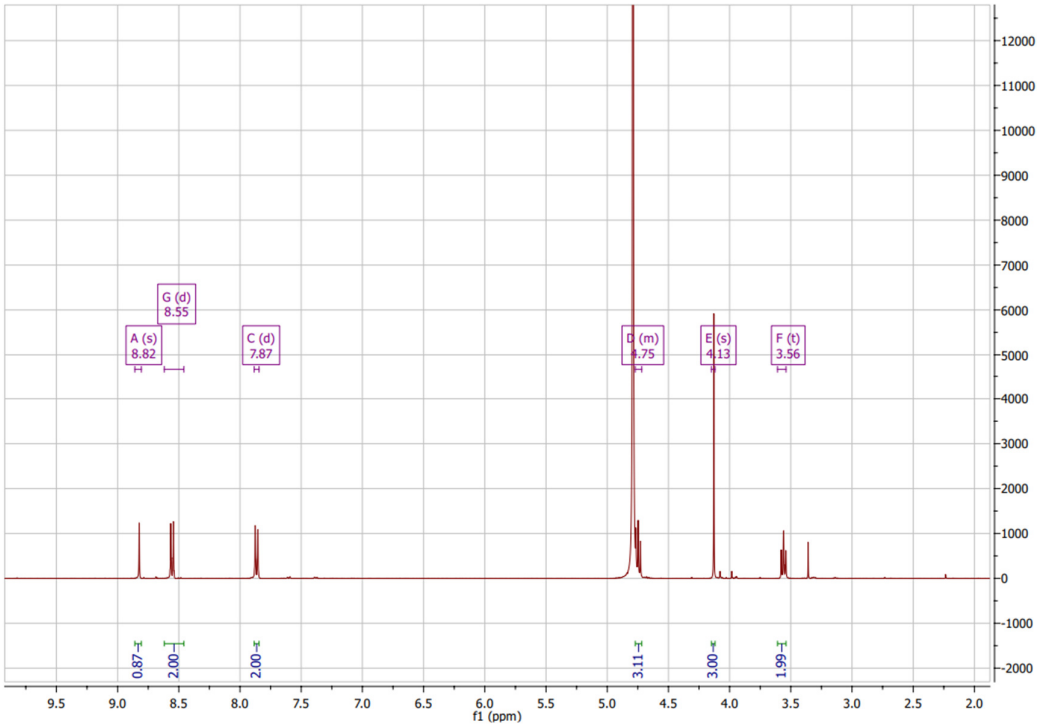

Figure S22. *^{1}H-NMR characterization of the formation of diazonium salt **4** in D_2O in which a clear shift is observed for the peaks in the aromatic region in comparison to the precursor **3** (Figure S16).*

Sources:

1. D. Channe Gowda, B. Mahesh and S. Gowda, *Indian J. Chem. - Sect. B Org. Med. Chem.*, 2001, **40**, 75.
2. R. A. G. Harmsen, A. Sivertsen, D. Michetti, B. O. Brandsdal, L. K. Sydnes and B. E. Haug, *Monatshefte fur Chemie*, 2013, **144**, 479.
3. L. Myles, N. Gathergood and S. J. Connon, *Chem. Commun.*, 2013, **49**, 5316.
4. G. B. Wang, L. F. Wang, C. Z. Li, J. Sun, G. M. Zhou and D. C. Yang, *Res. Chem. Intermed.*, 2012, **38**, 77.
5. J. Xiong, Y. Wang, Q. Xue and X. Wu, *Green. Chem.*, 2011, **13**, 900.
6. M. C. Rodríguez González, A. Brown, S. Eyley, W. Thielemans, K. S. Mali and S. De Feyter, *Nanoscale*, 2020, **12**, 18782.
7. N. Fairley, V. Fernandez, M. Richard-Plouet, C. Guillot-Deudon, J. Walton, E. Smith, D. Flahaut, M. Greiner, M. Biesinger, S. Tougaard, D. Morgan and J. Baltrusaitis, *Applied Surface Science Advances*, 2021, **5**, 100112.
8. A. G. Shard, *J. Vac. Sci. Technol. A*, 2020, **38**, 041201.
9. M.P. Seah, *Surf. Interface Anal.*, 2012, **44**, 1353.
10. M.P. Seah, *J. Electron Spectrosc. Relat. Phenom.*, 1995, **71**, 191.
11. B. Daelemans, S. Eyley, C. Marquez, V. Lemmens, D. E. De Vos, W. Thielemans, W. Dehaen and S. De Feyter, *Chem. Sci.*, 2022, **13**, 9035.
12. L. Liu, J. Bai, Z. Sun, Y. Yao, Z. Zhou, Y. Xia and Y. Zhang, *ACS Omega*, 2023, **8**, 16738.
13. L. Li, N. Yi, X. Wang, X. Lin, T. Zeng and T. Qiu, *J. Mol. Liq.*, 2018, **249**, 732.
14. Z. Sharifi, N. Daneshvar, M. S. N. Langarudi and F. Shirini, *Res. Chem. Intermed.*, 2019, **45** 4941.
15. R. H. Stadler, F. Robert, S. Riediker, N. Varga, T. Davidek, S. Devaud. T. Goldmann, J. Hau and I. Blank, *J. Agric. Food. Chem.*, 2004, **52**, 5550.